Table 1 Truss design—nonprestressed case

Member	Area (in.²)	Stress, Load 1 (ksi)	Stress, Load 2 (ksi)
1	0.797	19.76*	−5.33
2	0.416	14.44	14.44
3	0.797	−5.33	19.76*

presented by Schmit,[1] and contains many of the characteristics of the general minimum-weight structural design problem.

The truss has the geometry specified, and is subjected to the two independent load conditions indicated in the figure. The behavior is assumed to be of the linearly elastic-small deflection type, and buckling of the individual elements is not considered. For the nonprestressed case, the design variables are the cross-sectional areas of the three components. The objective function is linear, and twelve nonlinear behavioral constraints can be generated by a requirement that $-15 \text{ ksi} \leq \sigma_{ij} \leq 20 \text{ ksi}$; i.e., $\sigma_y = 20$ ksi for tension and 15 ksi for compression. Three side constraints specifying that the design variables be non-negative are also required.

The results of the optimum design of this structure are shown in Table 1. Using a material density of 0.01 lb/in.³, this design corresponds to a weight of 2.670 lb. Note that only two constraints are active for this design: those on yielding in tension of members 1 and 3 in loading condition 1 and 2, respectively. These critical stresses are noted in Table 1 with asterisks.

If the components of the truss of Fig. 1 are now assumed to be each precompressed by tension cables, three more design variables must be considered, namely the prestress in members 1, 2, and 3. Thus, the constraints of the preceding example must be modified as in Eq. (3), and six additional constraints of the form of Eq. (4) are required. These latter constraints state that the prestresses must be bounded by $-15 \text{ ksi} \leq \hat{\sigma}_i \leq 0$ since positive prestressing is not possible.

The results of this design are shown in Table 2. Weight is equal to 1.796 lb which constitutes a 33% reduction from the previous case. In this design, four constraints are binding at the optimum.

For the final example, consider the truss of Fig. 1 prestressed by an initial lack of fit of the three components. The additional design variables are now the changes in length (from nominal) of each member necessary to prestress the structure. For this case $\hat{\sigma}_y$ is taken equal to σ_y in both compression and tension.

Table 3 shows the final design, which has a weight of 2.226 lb. This design is fully stressed in both loading conditions and is 9% lighter than the optimal nonprestressed truss of Table 1. The existence of such a fully stressed design, made feasible by prestressing, was indicated in Ref. 2.

All numerical results presented above were obtained using an algorithm suggested by Fiacco and McCormick,[3] which transformed the problem of Eq. (5) into an unconstrained minimization problem. The penalty function $P(\mathbf{X},r_p)$ was minimized for each unconstrained cycle by the Variable Metric Method.[4,5] The initial value r_1 was computed using criterion 1 of Ref. 3 and subsequent values of r_p were calculated from $r_{p+1} = r_p/2$. For the example of Table 1, thirteen unconstrained cycles were executed; for design 2, ten cycles; and for design 3, twenty-one cycles. Design 2 was stopped somewhat short of full convergence. All examples used as the initial design $A_1 = A_3 = 2.0$, $A_2 = 1.0$ and zero prestress.

Table 2 Truss design—prestressed with cables

Member	Area, in.²	Prestress, ksi	Stress, load 1, ksi	Stress, load 2, ksi
1	0.609	−11.55	18.88*	−14.00*
2	0.075	−11.01	16.98	16.98
3	0.609	−11.55	−14.00*	18.88*

Table 3 Truss design—prestressed by lack of fit

Member	Area, in.²	Change in length, in.²	Prestress, ksi	Stress, load 1, ksi	Stress, load 2, ksi
1	0.573	0.0596	−4.42	19.98*	−14.96*
2	0.606	−0.0651	5.98	19.96*	19.96*
3	0.573	0.0596	−4.42	−14.96*	19.98*

References

[1] Schmit, L. A., "Structural Design by Systematic Synthesis," *Proceedings of the 2nd National Conference on Electronic Computation*, American Society of Civil Engineers, 1960.

[2] Dayaratnam, P., and Patnaik, S., "Feasibility of Full Stress Design," *AIAA Journal*, Vol. 7, No. 4, April 1969, pp. 773–774.

[3] Fiacco, A. V. and McCormick, G. P., "Computational Algorithm for the Sequential Unconstrained Minimization Technique for Nonlinear Programming," *Management Science*, Vol. 10, No. 4, July 1964, pp. 601–617.

[4] Davidon, W. C., "Variable Metric Method for Minimization," *Argonne National Laboratory*, Chicago, 1959.

[5] Fletcher, R. and Powel, M. J. D., "A Rapidly Convergent Descent Method for Minimization," *Computer Journal*, Vol. 6, 1963, pp. 163–168.

Cross-Hatching: A Material Response Phenomena

Ronald F. Probstein* and Harris Gold†

Avco Systems Division, Wilmington, Mass.

Model

One of the most intriguing and least understood fluid mechanical problems to have arisen over the past several years is that of "cross-hatching."[1–4] The term crosshatching refers to the spatially fixed diamond shaped patterns which have been observed to form on the surfaces of ablating bodies exposed to a supersonic turbulent or transitional boundary-layer flow. That the crosshatching appears on ablating surfaces has led to the idea the patterns might result from an interaction between the ablated material and the external supersonic flow (see, e.g., Ref. 4). Since some ablating materials melt, Nachtsheim[5] has also suggested that surface tension may be responsible for the formation of the patterns. We believe that ablation per se is not responsible for the origin of the cross-hatching but rather that the observed characteristic patterns result from the fact that materials which ablate become inelastic deformable relaxing and creeping bodies prior to ablating.

The model considered here is the response of an anelastic surface to the pressure fluctuations induced by a supersonic turbulent boundary layer leading to the cross-hatching as a consequence of a differential deformation due to a relaxation within the material. The patterns are not initiated as a result of differential ablation and can form in the absence of ablation. The pattern wavelength imposed on the material by the gaseous boundary layer λ must be of the order

Received October 15, 1969; revision received October 29, 1969. This work was sponsored by the Air Force Space and Missile Systems Organization under the Advanced Ballistic Reentry Systems Program Contract FO4-701-69-C-0117.

* Consultant; also Professor of Mechanical Engineering, Massachusetts Institute of Technology, Cambridge, Mass. Fellow AIAA.

† Senior Consulting Scientist. Member AIAA.

of $U\tau$, where U is a characteristic velocity within the boundary layer and τ a characteristic relaxation time for the material. This implies that the pattern geometry is independent of position on the model and that the patterns will form when the material relaxation time becomes comparable with an appropriate characteristic flow time. The problem as considered here is one of "natural" instability and is not concerned with artificially induced disturbances such as those caused by surface concavity, isolated roughness elements or holes, etc., any of which could influence the pattern geometry.

Outline of Stability Analysis

A two-dimensional, linearized stability analysis is carried out based on the assumption that the amplitude of the responding surface is sufficiently small that only small perturbations are induced in the flow. The boundary-layer flow is taken to be "nearly parallel" in the direction of the x axis, i.e., the velocity and temperature variations in the basic flow are functions of, at most, the normal direction y. For simplicity we here represent the turbulent boundary layer as having a uniform supersonic profile independent of y.

If both spatial and temporal perturbations are admitted the pressure disturbance field p' can be shown to be governed by the equation

$$(1 - M^2)\frac{\partial^2 p'}{\partial x^2} + \frac{\partial^2 p'}{\partial y^2} = \frac{M^2}{U^2}\frac{\partial}{\partial t}\left[\frac{\partial p'}{\partial t} + 2U\frac{\partial p'}{\partial x}\right] \quad (1)$$

where U is the basic local uniform flow velocity and M the corresponding Mach number. The disturbance velocity v' is related to the pressure field through the normal momentum equation

$$\rho Dv'/Dt \equiv \rho[\partial v'/\partial t + U\partial v'/\partial x] = -(\partial p'/\partial y) \quad (2)$$

where ρ is the local boundary-layer density. The boundary conditions far from the wall are that the pressure field is bounded and all waves propagate outwards.

It is, of course, the boundary conditions at the surface which introduce the material response since at the wall $y = \delta$ the normal velocity is continuous,

$$v' = D\delta/Dt \quad (3)$$

and its value is determined by the local surface deformation.

For simplicity we shall assume the surface to be a linear anelastic body[6] (Kelvin solid) recognizing, however, that, depending upon the material being considered, other relaxation and creep relations governing the material response[6] might be more appropriate. For a Kelvin solid, the defining equation

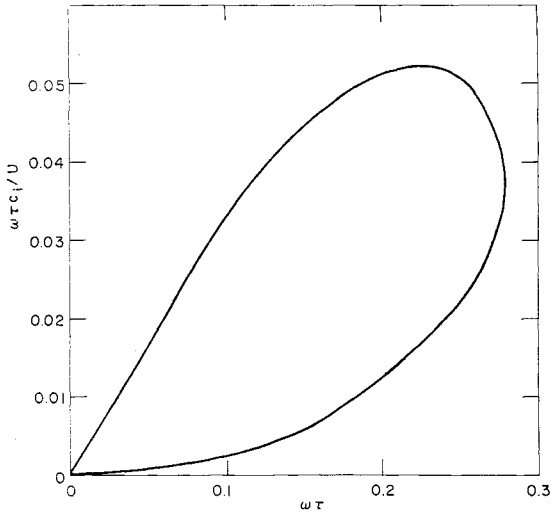

Fig. 1 Amplification rate vs frequency ($M^2 = 1.2$).

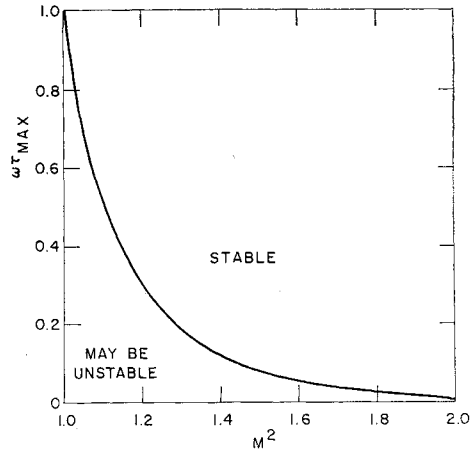

Fig. 2 Maximum frequency vs local effective Mach number.

for the strain E is

$$\tau(dE/dt) = E_{equil} - E = \sigma/2G - E \quad (4)$$

where σ is the stress in the solid, G the shear modulus, and τ the relaxation time equal to μ/G, with μ the viscosity of the solid. The local surface deformation can thus be related to the fluctuations in shearing stress through the relaxation equation

$$\tau(De'/Dt) = e'_{equil} - e' \quad (5a)$$

Here $e' = \partial\delta/\partial x$ is the local strain fluctuation (for $\lambda \gg \delta$), the equilibrium value of which is

$$e'_{equil} = \sigma'/2G = (\partial E_{equil}/\partial p)p' = \kappa p' \quad (5b)$$

σ' denoting the local fluctuation in shearing stress and κ a parameter measuring the proportionality between the fluctuations in pressure and shear stress. Identifying the gaseous shear stress at the wall with σ, it follows that for compressible turbulent flows for which $\sigma \sim p^{4/5}$

$$\kappa = \tfrac{2}{5}\gamma M^2(c_f/2G) \quad (6)$$

where p is the local pressure in the boundary layer and c_f the turbulent skin-friction coefficient defined with respect to the local dynamic pressure.

The solution to the stability problem specified by Eqs. (1) and (2) subject to the boundary conditions (3) and (5) is obtained in the usual manner by determining solutions for p' and v' which are periodic in x and t and then seeing whether these solutions amplify or decay. In the present analysis the phase velocity of the disturbance is zero since the wave pattern is stationary.

Results and Comparison with Experiment

Some results of the analysis described previously are presented in Figs. 1 and 2. Figure 1 is a stability curve for a Mach number $M = (1.2)^{1/2}$. The disturbance frequency $\omega = 2\pi U/\lambda$, where λ is the disturbance wavelength and the imaginary part of the complex phase velocity of the disturbance c_i is the amplification factor. Each point on the curve of Fig. 1 corresponds to a different value of the parameter κ[Eq. (6)]. Thus for a given value of κ there is only one frequency for which there is amplification, i.e., κ determines the flowfield frequency (or wavelength) for which there is resonance. In Fig. 2, the maximum frequency is shown as a function of the local Mach number, and it can be seen that instability can occur only in the limited Mach number range $1 \leqslant M^2 \leqslant 2$.

From Fig. 2, it is seen that an instability can set in for $\omega\tau \sim 0(1)$ or for a wavelength $\lambda \sim U\tau$, as noted earlier. In other words, for a fixed characteristic velocity the pattern spacing

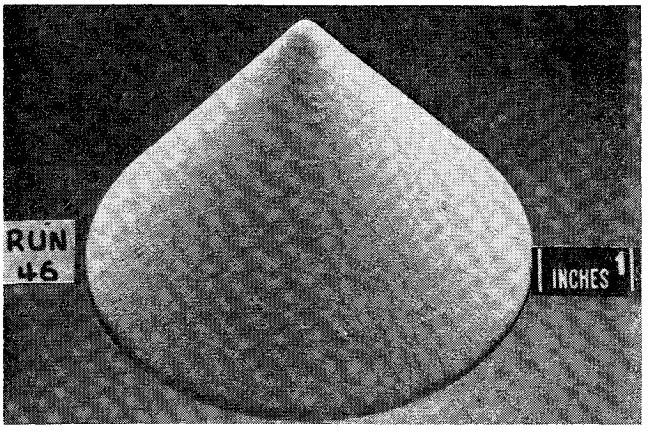

Fig. 3 Teflon (FEP) cone which experienced material creep but which did not ablate during supersonic wind-tunnel experiment carried out by P. R. Nachtsheim (white paint used to accentuate crosshatching). Photograph courtesy NASA Ames Research Center.

should be independent of position on the body or size of the body and should depend only on the material relaxation time. Ballistic range experiments by Canning et al.[2] on ablating Lexan cones of about 0.4-in. slant height led to pattern wavelengths of 0.01–0.02 in., while wind-tunnel tests by Larson and Mateer[3] on ablating Lexan cones with slant heights around 5 in. led to wavelengths of 0.05–0.07 in., an average factor of 4 change in wavelength with more than a factor of 10 change in body size. However, the wavelength change can be accounted for by the different test temperature conditions resulting in a larger value for τ in the wind-tunnel case. Wind-tunnel tests have been run at the Avco Systems Division on ablating Teflon wedges 2 in. in length and the measured wavelengths are about 0.4 in. During the course of the investigation analysis was also made of recovered reentry flight test vehicles made of Teflon which were 30–40 in. long and wavelengths were found to be in the range 0.3–0.4 in., indicating an essentially unchanged wavelength for a factor of 20 change in body size. The observed wavelengths are consistent in order of magnitude with a relaxation time $\tau \sim 10^{-5}$ sec and a velocity $U \sim 2 \times 10^3$ fps. Data on τ are not readily available but data on G and estimates of μ give the indicated value of τ.

The theoretical result that instability arises for $1 \leqslant M^2 \leqslant 2$ is consistent with the experimental findings that the boundary layer must be turbulent for crosshatching to occur and that the pattern angle closely follows the Mach angle corresponding to the local boundary-layer edge Mach number up to about 2.5–3.0 and then "freezes" out for all higher values.[4] For a turbulent boundary layer at low supersonic Mach numbers the profile is almost uniformly supersonic at a value close to the edge Mach number except immediately adjacent to the wall within the sublayer. On the other hand, at high supersonic Mach numbers in the region of the sublayer edge the Mach number tends to "freeze" out at a value around 2–3.[4] This leads to a characteristic "effective" Mach number within the boundary layer of, say, 1–2. It may be appropriate in considering the three-dimensional pattern to identify this Mach number with that normal to the wavefront.

A Critical Experiment

If the model of the present Note were correct then a nonablating inelastic deformable body could, when placed in supersonic turbulent flow, give rise to crosshatching. P. R. Nachtsheim in cooperation with H. K. Larson of the NASA Ames Research Center kindly agreed to carry out such an experiment in the Ames 3.5-ft Hypersonic Wind Tunnel (see Ref. 3 for a description of the tunnel). The model tested was a 40° half-angle Teflon (FEP) cone of 5 in. base diameter. The material properties were such that at the test conditions of 1673°R stagnation temperature and 1582 psia stagnation pressure and for the 7-sec test time the body did not ablate (either sublime or form a discernible liquid melt) but did exhibit creep. The freestream Mach number was 7.4 and the Mach number at the edge of the boundary layer was 2. The boundary layer itself was turbulent.

When the test was begun nothing was seen to happen for the first few seconds, during which time the model heated up. After this period, however, the material has softened sufficiently and a crosshatch pattern was observed to break out simultaneously over the entire length of the model. When removed from the tunnel the model showed no mass loss to within the measurement accuracy of 0.1 g for the 650 g cone, the pattern angle was consistent with previous measurements (~35°), while the pattern wavelength was around 0.1 in. A photograph of the unablated but crosshatched model is shown in Fig. 3. The blotches seen in the photograph result from the fact that the model was painted white to accentuate the crosshatching.

Concluding Remarks

The results of the nonablating experiment are consistent with those for ablating bodies and lends strong support to the material response model outlined. It may be expected that some details of the model as described will require modification but the deformable relaxing and creeping surface should form the basis for any description of the phenomena.

References

[1] Wilkins, M. E., "Evidence of Surface Waves and Spreading of Turbulence on Ablating Models," *AIAA Journal*, Vol. 3, No. 10, Oct. 1965, pp. 1963–1965.

[2] Canning, T. N., Wilkins, M. E., and Tauber, M. E., "Ablating Patterns on Cones Having Laminar and Turbulent Flows," *AIAA Journal*, Vol. 6, No. 1, Jan. 1968, pp. 174–175.

[3] Larson, H. K. and Mateer, G. G., "Cross-Hatching—A Coupling of Gas Dynamics with the Ablation Process," AIAA Paper 68-670, Los Angeles, Calif., 1968.

[4] Langanelli, A. L. and Nestler, D. E., "Surface Ablation Patterns: A Phenomenology Study," *AIAA Journal*, Vol. 7, No. 7, July 1969, pp. 1319–1325.

[5] Nachtsheim, P. R., "Analysis of the Stability of a Thin Liquid Film Adjacent to a High-Speed Gas Stream," TN D-4976, Jan. 1969, NASA.

[6] Freudentahl, A. M., *The Inelastic Behavior of Engineering Materials and Structures*, Wiley, New York, 1950, pp. 220–231, 305–356.

Linearly Exact Transverse Displacement Variation

T. J. Kozik*
Texas A&M University, College Station, Texas

Nomenclature

A,B = Lamé surface parameters for the undeformed reference surface
$e_{\alpha\alpha},e_{\alpha\beta},e_{\beta\beta}$ = tangential normal and shear strains
$e_{\alpha\gamma},e_{\beta\gamma},e_{\gamma\gamma}$ = transverse shearing strains and transverse normal strain
$\bar{i},\bar{j},\bar{k}$ = unit tangent vectors to the α and β coordinate curves of the undeformed surface and the unit normal to that surface

Received July 8, 1968; revision received October 27, 1969. The work reported was supported by NASA research grant NSG 44-001-031.

* Professor of Mechanical Engineering.